EXPERIMENTAL VALIDATION OF PIEZOELECTRIC ENERGY HARVESTING DEVICE FOR BUILT INFRASTRUCTURE APPLICATIONS

Paul Cahill[1,*], Alan Mathewson[2] and Vikram Pakrashi[3]

** Corresponding author. Email address: paul.cahill@ucc.ie*

ABSTRACT

Vibration energy harvesting devices are increasingly becoming more efficient and useful. The performance of such devices for energy harvesting from vibrations of civil infrastructure can be theoretically quantified and energy harvesting under harmonic loadings can be validated experimentally. Experimental validation of such devices for civil infrastructure applications, such as bridges, remain an important but more complex and challenging issue, in part due to the more uncertain nature of the dynamic response of structures under operational conditions and problems with access for such testing. Lack of existing experimental benchmarks is also a major obstacle behind adopting this technology for bridges. This study presents a laboratory based experimental procedure through which a piezoelectric energy harvester is experimentally verified for rail bridges in their operational condition with trains traversing them. A general experimental arrangement required for validating a cantilever energy harvesting device is presented along with the fabrication of a prototype device and detailed experimental setup. A model bridge undergoing loadings from an international train fleet is chosen and the acceleration response from the bridge is used as the excitation source for the energy harvesting device. Numerically estimated performances of the energy harvester are validated by experimentation for a range of trains. The method is applicable for validating energy harvesting from arbitrary vibrations of built infrastructure within the laboratory environment without the need of scaling. The device and related experimental procedure will serve as a benchmark for similar unscaled tests within a laboratory environment and can be useful for assessing devices or their applications in monitoring the built infrastructure under realistic conditions without the need of deployment in site.

[1] Paul Cahill. Centre for Marine and Renewable Energy Ireland (MaREI), Environmental Research Institute (ERI), University College Cork, Ireland.

[2] Alan Mathewson. Heterogeneous Systems Integration Group, Micro & Nano Systems Centre, Tyndall National Institute, Cork, Ireland.

[3] Vikram Pakrashi. Dynamical Systems and Risk Laboratory, School of Mechanical and Material Engineering and Centre for Marine and Renewable Energy Ireland (MaREI), University College Dublin, Ireland.

INTRODUCTION

Advances in microelectronic technology has created the opportunity for improved and efficient sensing of built infrastructure in their operational conditions and this can have a direct effect on their demand related to maintenance and management for degrading infrastructure networks (Znidaric et al. 2011). Wireless sensing for remote monitoring of infrastructure is becoming increasingly popular (Gungor and Hancke 2009) but challenges related to reliable power supply to such nodes is remain an important issue. Vibration energy harvesting devices (EHD) have the potential to act as a power source for such sensing nodes, through the conversion of ambient vibrations of the host structure into electrical energy (Anton and Sodano 2007). As a result, the optimization of the energy output from such harvesters is critical for the development of remote, self-supporting, wireless sensor networks (WSN's) (Shaikh and Zeadally 2016).

Such optimizations have resulted in vibration EHD becoming increasing efficient, with growing levels of power being generated from vibrational sources (Al-Ashtari at al. 2013). Advancements in material (Jackson at al. 2013), circuitry (Priya 2007) and design properties (Liu et al. 2012) have been shown experimentally to increase efficiency. These studies have been mainly conducted under harmonic loading conditions, which is not representative of real-world civil infrastructure systems, where the excitation can be more random. The optimisation of devices for such systems is not as well-researched, with the experimental validation of such being even less so (Chong and Kumar 2003). This is despite the significant potential such applications can offer (Zuo and Tang 2013). By integrating vibration EHDs, such as electro-magnetic (Sazonov et al. 2009) and piezoelectric (Erturk 2011), with civil infrastructure, the conversion of the vibrational response of the structure to electrical energy can be achieved with no impact on the operational performance of the structure. While a number of different civil infrastructure have been proposed as appropriate candidates for energy harvesting, such as tunnels (Wischke et al. 2011) and high-rise buildings (Xie at al. 2013), the majority of studies have investigated bridges. In this regard, the application of piezoelectric EHDs with bridge infrastructure under operational conditions has been investigated for train (Cahill et al. 2014b) and highway bridges (Ali at al. 2011), with the life-cycle effects on such devices similarly being considered (Cahill et al. 2016a).

While the aforementioned studies have proven the feasibility of using vibration EHDs with civil infrastructure from a theoretical viewpoint, experimental validation is often lacking. There have been some studies on the use of piezoelectric EHDs as a means of detecting damage when integrated with concrete beams, both for surface mounted devices (Cahill et al. 2014a) and embedded devices (Kaur and Bhalla 2016). However, the loading conditions considered were not representative of real world scenarios, including the study considering a laboratory test of a scaled bridge structure for energy harvesting (Kim et al. 2011). Real-world applications have

received some attention; including the integration of piezoelectric EHD with a highway bridge (Peigney and Siegert 2013) and a train bridge (Kołakowski at al. 2011). While such studies established the potential for structural applications of EHDs under operational conditions, full-scale experiments are difficult to be carried out or even considered due to complexity, access aspects, safety and costs associated with such large experiments.

An alternative to full-scale testing is to develop a laboratory based testing procedure by using the theoretical or measured vibration responses of civil structures as the vibrational excitation signal applied to the EHD. Initial research on such an approach has been shown to be an effective in investigating applications of cantilever based piezoelectric EHDs with seismic sources (Elvin at al. 2006) and a bridge application under operational conditions (Cahill et al. 2016b). Considering the fact that the magnitudes of dynamic displacements are not very large and the accelerations are limited to usually less than 0.5G, there remains an opportunity to use simulated, synthetic or historic real data in a vibration shaking table without scaling as an input to excite EHDs.

This paper presents a laboratory based experimental technique for validation of piezoelectric energy harvesting devices connected to built infrastructure in their operational condition without having to access the site of the built infrastructure. A model for a cantilever based EHD is provided, along with the fabrication, experimental setup and calibration of a prototype device. A train bridge is chosen for demonstration, with details of the model bridge undergoing operational loading conditions from an international train fleet provided. Dynamic responses due to train passages on the model bridge provide excitation to the EHD. Numerical estimates of energy harvested are compared with experimental results obtained from laboratory experiments. The voltage outputs from the EHD are analyzed and compared, along with the acceleration responses of the host structure via numerical and experimental comparisons to demonstrate the suitability and accuracy of the proposed laboratory based experimental procedure.

PIEZOELECTIC ENERGY HARVESTING DEVICE

Piezoelectric EHDs generate electrical energy through the conversion of fluctuations in the strain applied to the active piezoelectric materials within the devices. This electro-mechanical behavior can be expressed through the linear fundamental relationship represented by (IEEE 1988)

$$S_p = s_{pq}^{E} T_q + d_{kp} E_k \tag{1}$$

$$D_i = d_{ip} T_q + \varepsilon_{ik}^T E_k \tag{2}$$

which can be subsequently rewritten in matrix form for convenience as

$$\begin{bmatrix} S_p \\ D_i \end{bmatrix} = \begin{bmatrix} s_{pq}^E & d_{kp} \\ d_{iq} & \varepsilon_{ik}^T \end{bmatrix} \begin{bmatrix} T_q \\ E_k \end{bmatrix} \tag{3}$$

where S is the strain vector, D is the electric displacement vector, s^E is the elastic compliance matrix under constant electric field, denoted by ^{E}, d is the piezoelectric constant matric, ε^T is the permittivity matrix under constant stress, denoted by ^{T}, T is the stress matrix and E is the electric field matrix. These relationships can be used to establish the electrical response of the piezoelectric material from strain fluctuations imposed upon it due to the vibration response of the host structure.

A common piezoelectric EHD is a cantilever, consisting of a piezoelectric material attached to a cantilever substrate, which is attached via a rigid base to the designated host structure [Fig. 1(a)]. The piezoelectric material, with bound electrodes to transport charge from the material, is bonded to the cantilever substrate, which most often has an affixed tip mass located at the free end of the beam, [Fig. 1(b)], to allow for frequency optimization (Wang and Meng 2013).

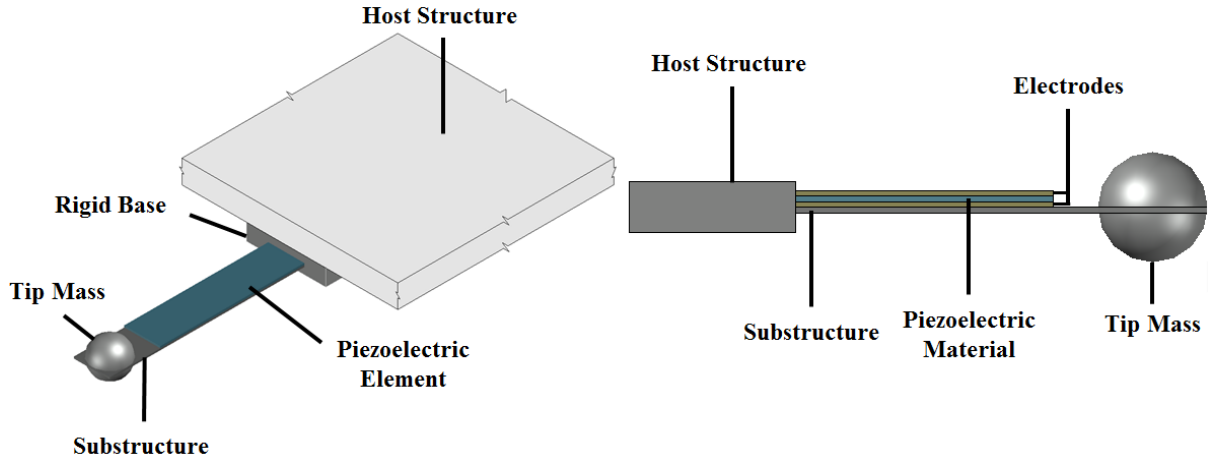

Fig. 1. Illustration of piezoelectric cantilever based EHD (a) Attached to host structure and (b) Side elevation of the device

The cantilever is embedded within a rigid fixed base mounted onto the host structure of interest for structural applications, with the acceleration response of the host providing the base excitation to the device. The electromechanical behaviour of the cantilever energy harvester can be expressed by (DuToit and Wardle 2007)

$$m_c \ddot{z} + c_c \dot{z} + k_c z - \theta V = -m_c \ddot{y}_b \tag{4}$$

$$\theta \dot{z} + C_p \dot{V} + \frac{1}{R_l} V = 0 \tag{5}$$

where m_c, c_c and k_c are the mass, damping and stiffness of the energy harvester respectively and z is the relative displacement of m_c, with over-dots denoting differentiation with respect to time and y_b is the base acceleration from the host structure. The electromechanical coupling coefficient is given as θ, V is the voltage and C_p and R_l are the capacitance and load resistance respectively. The natural frequency, ω_c and the damping factor, ξ_c, of the harvester are defined as

$$\omega_c = \sqrt{\frac{k_c}{m_c}} \quad and \quad \xi_c = \frac{c_c}{2 m_c \omega_c} \tag{6}$$

EXPERIMENTAL PIEZOELECTRIC DEVICE FOR STRUCTURAL APPLICATIONS

Piezoelectric EHD Validation Protocol for Structural Applications

For determining the performance of a vibration EHD for structural applications in a laboratory environment, knowledge of the dynamic response of the host structure under operational conditions is required. Such responses can be acquired through either appropriate theoretical analysis or through experimental analysis whereby the response of the structure is measured in the field (Pakrashi et al. 2013). The dynamic responses obtained are subsequently applied to the appropriate EHD, with acceleration profiles from the host forming the base excitation to cantilever based EHD. In this manner, devices can be experimentally validated for applications for any structure providing the response datasets are available. The protocol, therefore, for such validation is as follows:

1. Theoretical Benchmarking: Determining the theoretical performance of the designed EHD when integrated with a host structure, by using the suitably identified theoretical or measured datasets as the excitation applied to the device.

2. Fabrication of Device: Fabrication of an experimental prototype of the proposed EHD, based on design and theoretical specifications.

3. Experimental Calibration: This is required if certain parameters of the energy harvester require experimental validation, with harmonic loading conditions being applied to the experimental prototype.

4. Experimental Validation: The validation of the prototype EHD through the application of theoretical or measured datasets of the dynamic response of the host structure as the excitation source.

Unlike Step 4, the first three steps have been well established in previous studies, as detailed in the introduction. This final step provides the experimental validation for individual devices for specific structural applications, the dynamic response of which is most often not harmonic in nature under operational conditions. Therefore, the experimental validation requires careful attention and consideration in order to yield reliable experimental estimates of the EHD outputs for large-scale civil infrastructure. The following sections outlines the datasets used to validate structural applications, the experimental creation and setup required to experimentally validate cantilever based EHD.

Host Structure for Piezoelectric Energy Harvesting Device

The host structure chosen for this study is a model train bridge undergoing operational loadings from an international train fleet. The solid section 3-dimensional bridge, of length 10.6*m* and width 10m, was created using the finite element software Strand 7 and consists of two railway tracks supported by concrete sleepers atop of the reinforced-concrete, slab and girder bridge. The properties of the model bridge's slab and girders are provided in Table 1, with more complete details on the creation and solving of the model are available in (Cahill et al. 2014b).

Parameter		**Value**
Length, **(**m)	$\boldsymbol{L}$	*10.6*
Width (m)	$\boldsymbol{B}$	*10.0*
Damping Ratio (%)	$\boldsymbol{c}$	*2.15*
Young's Modulus (N/m^2)	$\boldsymbol{E}$	38×10^9
Density (kg/m^3)	$\boldsymbol{\rho}$	*2400*
Second Moment of Area (m^4)	$\boldsymbol{I}$	*33.366*
Cross Sectional Area (m^2)	$\boldsymbol{A}$	*4.4*
Natural Frequency (Hz)	$\boldsymbol{\omega_n}$	*12.10*

Table 1. Properties and dimensions of model train bridge.

Considering traffic over the bridge, a train fleet was modelled comprising of five different train sets with an international geographical spread, including the Irish diesel classes 071Loco and 201Loco, the electrical French TGV, the German ICE and the Japanese Shinkansen. Each trainset was modelled with realistic operational locomotive and carriage configurations, loadings and spacing, with details of the fleet provided in Table 2.

	071Loco	201Loco	TGV	ICE	Shinkansen	Unit
Number Locomotives	1	1	2	2	2	
Locomotive Length	17.4	21.0	22.2	20.2	26.1	m
Number Carriages	7	7	10	12	14	
Carriage Length	23.0	23.0	18.7-21.9	26.4	25.0	m
Locomotive Axle Load	161.9	182.5	158.3	190	107.3	kN
Carriage Axle Load	117.7	117.7	158.3	140	107.3	kN
Total Train Length	178.4	182.1	237.6	357.1	402.1	m
Total Train Load	4,267	4,391	4,748	8,240	6,867	kN

Table 2. Characteristics of international train fleet for passage over model bridge.

The primary focus of this study is to determine, both theoretically and experimentally, the performance of a piezoelectric EHD arising from its coupling with the model train bridge. In this regard, the dynamic response from the bridge due to vehicle passage was obtained. Each train was modelled so as to complete a single passage of the bridge at a speed of 100 km/hr and the acceleration response at the mid-span of the bridge determined [Fig. 2]. As can be seen, the different train loadings, axle spacing and configurations results in bridge responses of different magnitudes and durations, with the highest magnitude output due to the 201Loco locomotive, whereas the longest response was obtained for the Shinkansen due to it being the train with the greatest length. For each passage, a time duration of 5 seconds was included after the train had completed its passage in order to capture the damping of the bridge due to free vibration. Using the obtained acceleration profiles, the theoretical voltage output from a cantilever EHD can be obtained by using the acceleration responses as the base excitation to Eq. 4 and Eq. 5. By applying arbitrary responses through an appropriate dynamic experimental setup, they provide the base excitation to porotype EHD and can validate experimentally the performance of such devices with specific built infrastructure applications.

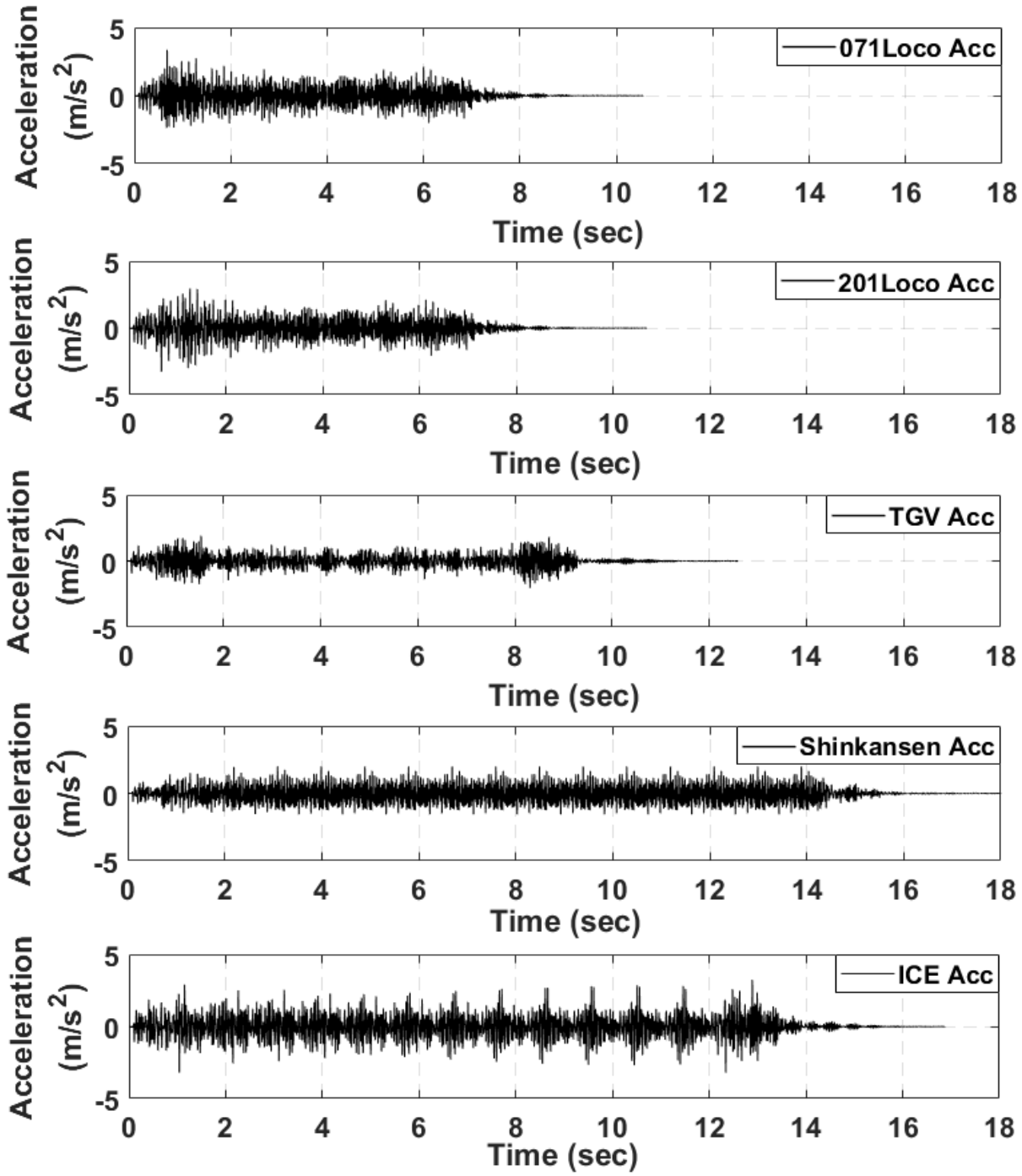

187 Fig. 2. Acceleration outputs from finite element model bridge under international train loadings
188 including 071Loco, 201Loco, TGV, Shinkansen and ICE.

189 **Fabrication of Experimental Piezoelectric EHD**

190 For the fabrication of the cantilever based EHD experimental prototype, the piezoelectric
191 material chosen was PolyVinyleDene Fluoride (PVDF) of thickness 52μm with silver elec-
192 trodes. PVDF is a polymer material, which results in high mechanical strength while retaining
193 excellent flexibility (Anton and Sodano 2007), resulting in a material which is highly adaptive
194 to a variety of conditions and applications. A PVDF harvester, measuring 50mm in length and

20mm in width, was created with attached electrodes to carry the charge developed within the material, with the material properties of the material provided in Table 3.

Parameter		Value
Length (m)	l_h	*0.05*
Width (m)	b_h	*0.02*
Capacitance (nF)	C_p	*1.966*
Modulus of Elasticity (N/m^2)	E_h	*8.3 x 10^9*
Piezoelectric Constant (C/m^3)	e_{31}	*0.1826*
Resistance (kΩ)	R_l	*1000*

Table 3. Properties of PVDF energy harvester bonded to cantilever substrate.

A cantilever substrate was subsequently created using an aluminium beam of thickness 1.25mm and width 25mm, onto which the PVDF harvester was bonded. In order to match the natural frequency of the EHD with that of the host structure at 12.10Hz, the length of the cantilever beam was set at 158mm and a tip mass of 0.03kg was subsequently attached to the free end of the beam. The cantilever was subsequently embedded within an aluminium base, consisting of two aluminium plates of length, width and thickness 50mm, 25mm and 3mm respectively. In order to provide a representative load to characterise a connected circuit, as would be the case for real-world applications whereby the harvester is connected to an energy storage or data transmission circuit, the electrodes of the harvester were connected to a variable resistor, set to a resistance of 1 MΩ.

Following the fabrication process, and in advance of experimentally investigating the EHD to determine its performance for structural application, it is first required to experimentally calibrate the EHD in order to experimentally verify key parameters.

Experimental Setup

A laboratory based experimental setup was created to apply unscaled acceleration profiles obtained from the train passages as the base excitation to the experimental prototype [Fig. 3]. These profiles were applied by a waveform generator, via an amplifier, to a vibration unit onto which the EHD has been attached. As the waveform generator, amplifier and vibrator unit create an output replicating the profile of the host structure but not the amplitude, a controller unit is required to allow the magnitude of the signal to be monitored and controlled. Therefore, a control unit monitoring the output was coupled with the vibration unit, with a continuous feedback loop to the input signal adopted so as to ensure agreement between the desired input signal and the experimental output. The voltage output from the EHD was simultaneously measured using an oscilloscope and its performance determined.

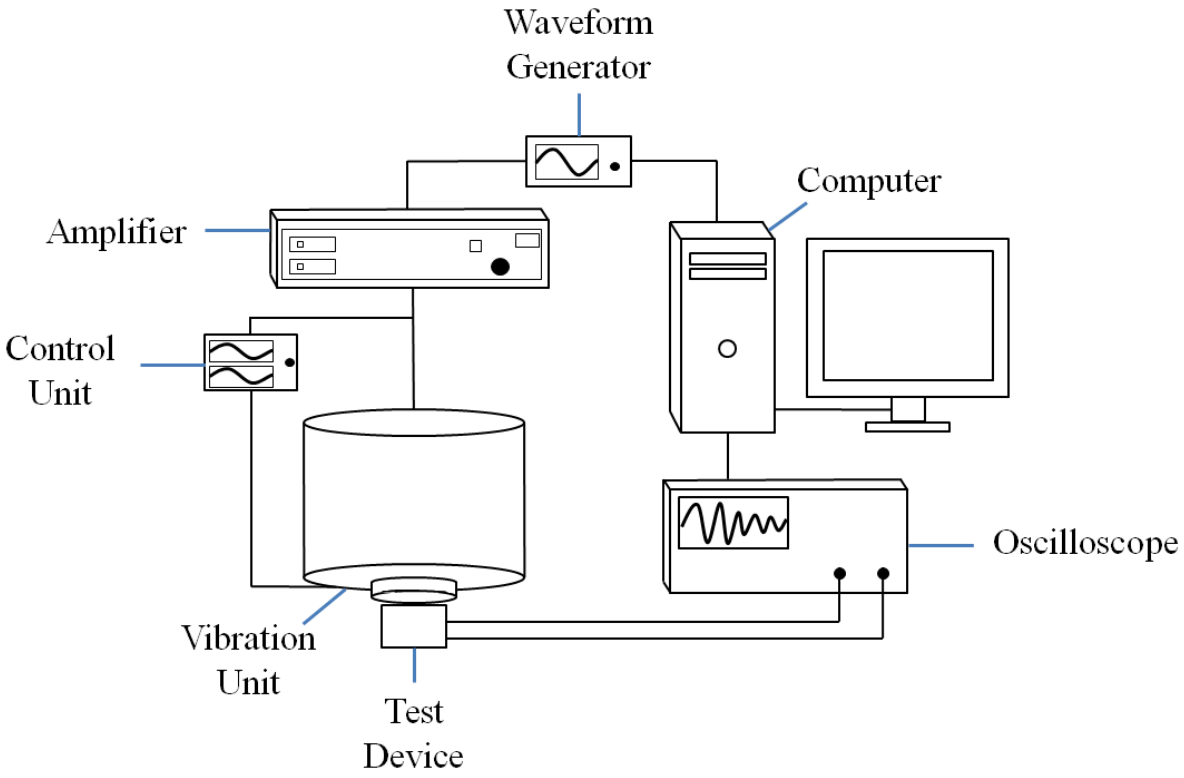

Fig. 3. Schematic of experimental set-up for the validation of piezoelectric EHD with civil infrastructure in a laboratory environment.

For the purposes of this experimental investigation, the vibration unit used was an LDS V455 Series permanent magnet shaker, with accompanying PA1000L Amplifier and a Digilent Inc. Analog Discovery waveform generator and oscilloscope. The control unit used was a MicroStrain G-Link 10G LXRS wireless triaxial accelerometer. The prototype EHD was attached alongside the accelerometer on the permanent magnet shaker, orientated so as to be applying the base excitation to the cantilever in the vertical plane [Fig. 4]. The use of the tri-axial accelerometer can be used as a further safeguard to ensure the experimental setup is functioning correctly when considering vibration testing of a cantilever EHD. The vibrations being applied to the EHD during such tests are on a single plane of motion and can be monitored using a uniaxial accelerometer. However, using a tri-axial accelerometer, accelerations outside of the plane of loading can be monitored to ensure that no out of plane vibrations are applied to the device.

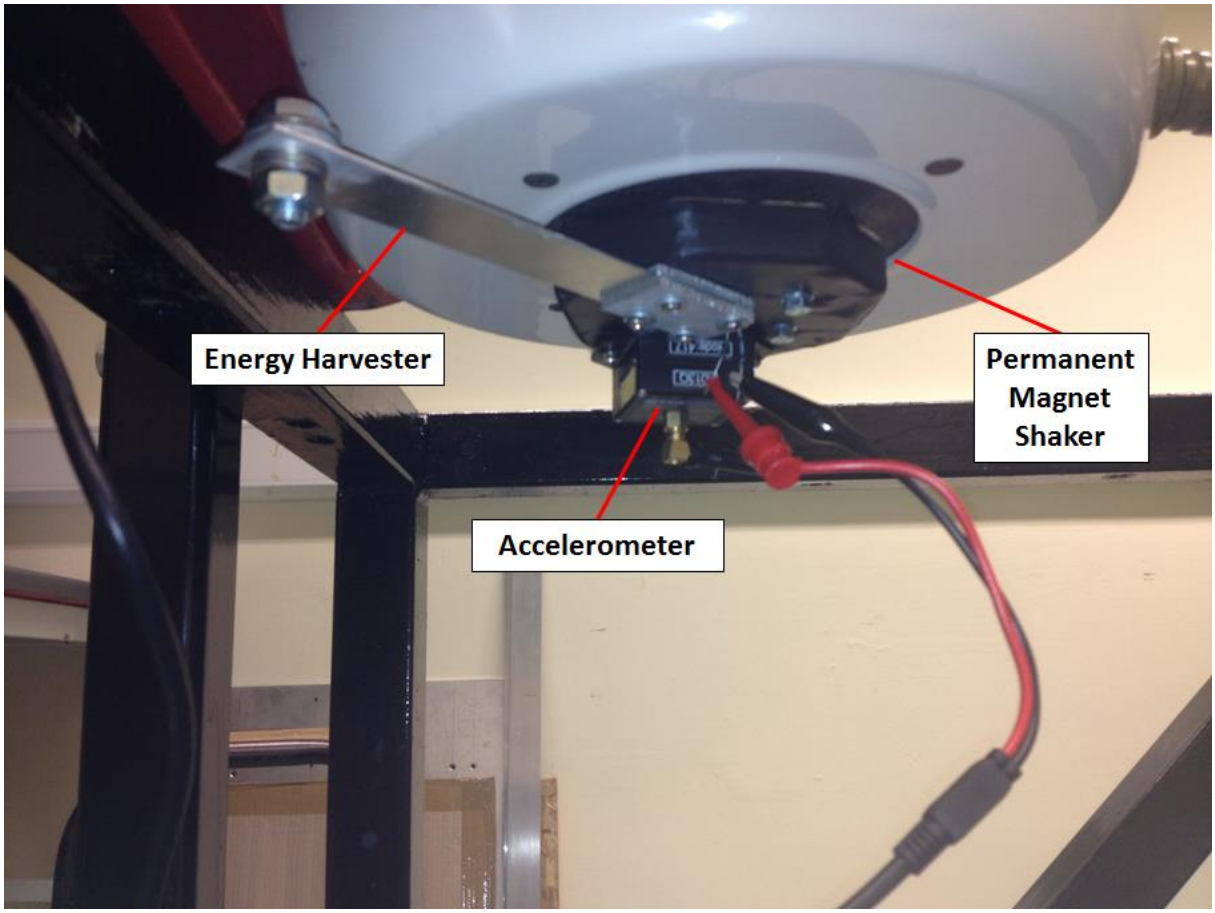

Fig. 4. Experimental setup for the validation of the cantilever EHD for structural applications.

EXPERIMENTAL RESULTS

Experimental Calibration of Prototype Device

To calibrate experimentally the cantilever EHD and verify its parameters, the response of the device under harmonic loading conditions was determined and compared against theoretical outputs. The harmonic loading consisted of sinusoidal base excitation at a constant magnitude of 0.5G acceleration (4.905m/s^2) with varying frequencies of loadings. The acceleration provided as the base excitation was monitored by the wireless accelerometer to ensure compliance with the required loading conditions, whilst the voltage was measured and compared against theoretical calculations. Fig. 5 illustrates an example calibration result, with theoretical acceleration being compared against experimental output being applied to the prototype, at a frequency of 13.4Hz, along with the corresponding theoretical and experimental voltages.

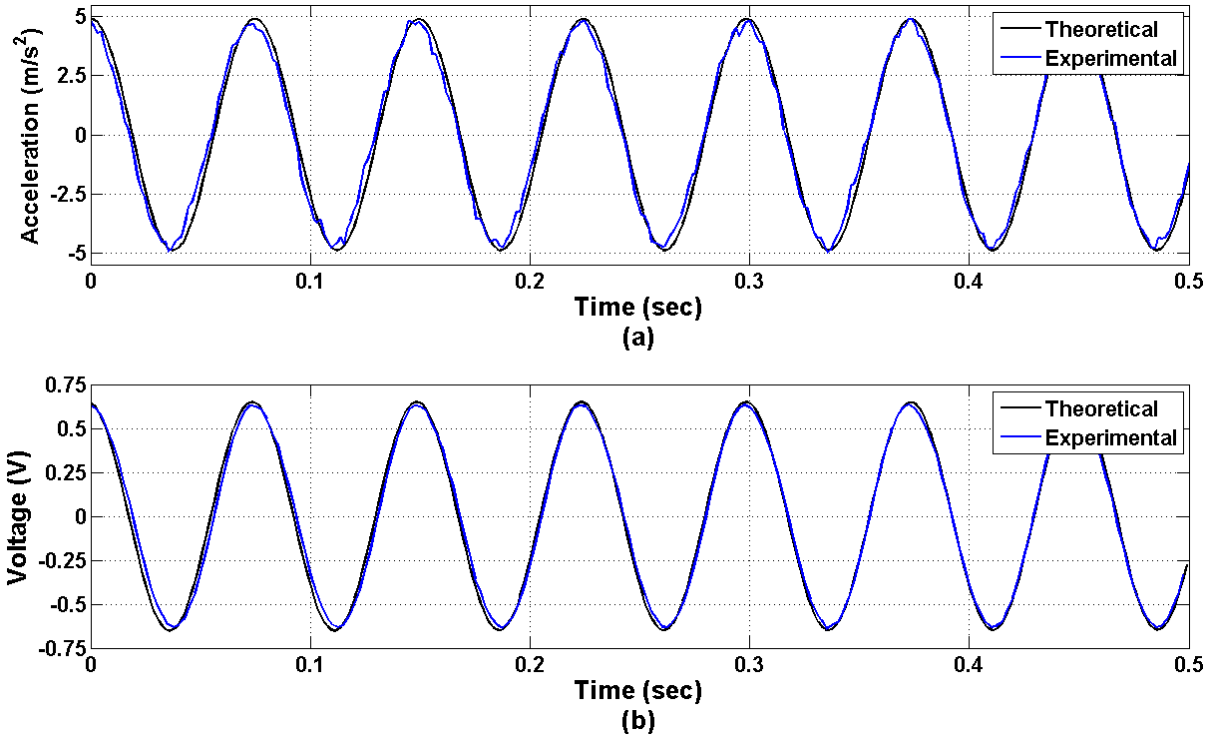

Fig. 5. Sample comparison of theoretical and experimental analysis of prototype at a loading frequency of 13.4Hz for (a) Acceleration and (b) Voltage.

As the natural frequency of the harvester was calculated to be 12.10Hz, a range of frequency loadings of between 8Hz and 17Hz were applied to the EHD. Taking the peak AC voltage at each loading frequency, it was found that while the experimental magnitudes corresponded with the predicted theoretical output [Fig. 6], with a natural frequency of the experimental prototype found to be 12.79Hz. The electromechanical coefficient was experimentally validated to be 1.289μC/m, with all verified parameters outlined in Table 4. This, combined with Eq. 4 and Eq. 5, allows for the experimental validation of the EHD and its comparison with theoretical predictions for structural applications.

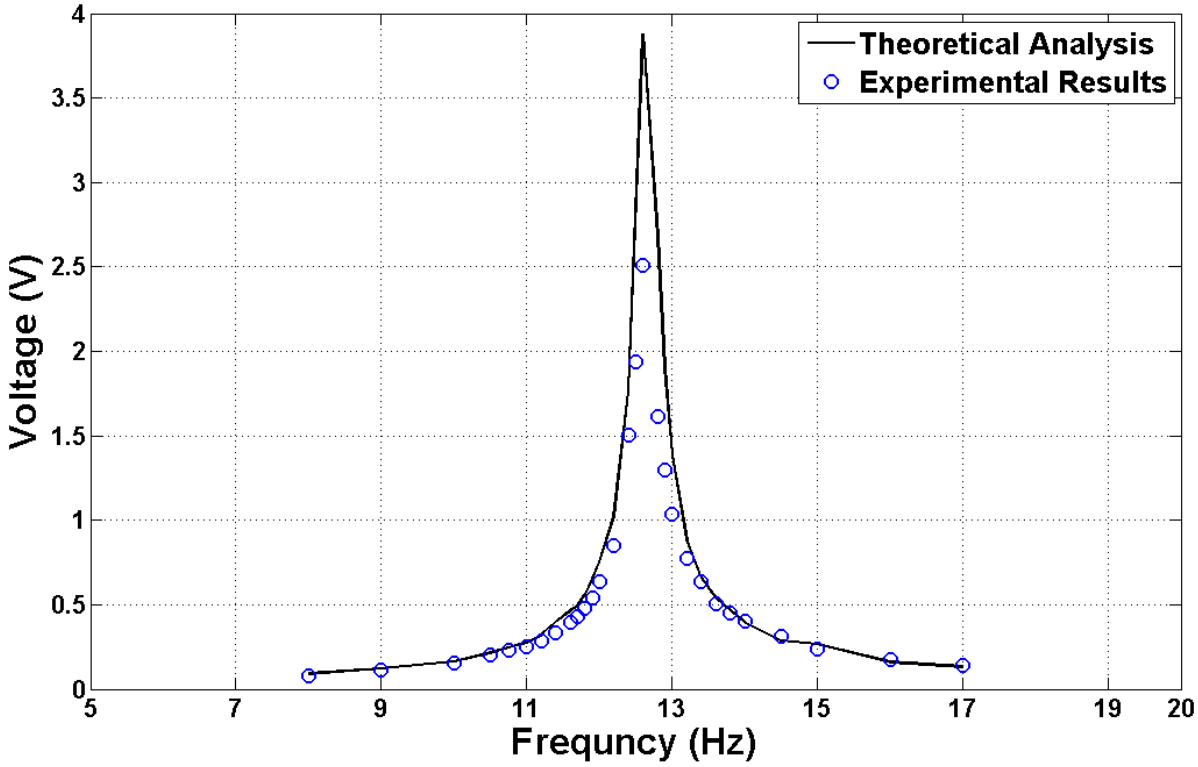

Fig. 6. Calibration curve of experimental EHD with the theoretically predicted voltage output compared against measured experimental voltage outputs.

Parameter		Value
Capacitance (nF)	C_p	1.966
Stiffness (N/m^2)	k_c	0.02
Damping Factor	ξ_c	0.04
Natural Frequency (Hz)	ω_c	12.79
Electromechanical Coefficient (μC/m)	θ	1.289

Table 4. Validated parameters for Experimental EHD.

Experimental Validation of Energy Harvesting Device

For experimental validation of the EHD for applications involving responses in operational conditions, the passage of the 071Loco train was selected first. The input acceleration profile and the theoretical voltage output were compared against their experimental counterparts. The input acceleration and the measured experimental acceleration, serving as the input to the EHD, correlated well [Fig. 7(a)]. The predicted voltage output of the cantilever EHD corresponded with the magnitudes of the experimental analysis [Fig. 7(b)]. The voltage output was theoretically predicted to have a smooth, uniform oscillation profile whilst the experimental analysis had noisy components. The voltage output from the theoretical prediction was $0.045V_{RMS}$, as compared to an experimental output of $0.037V_{RMS}$.

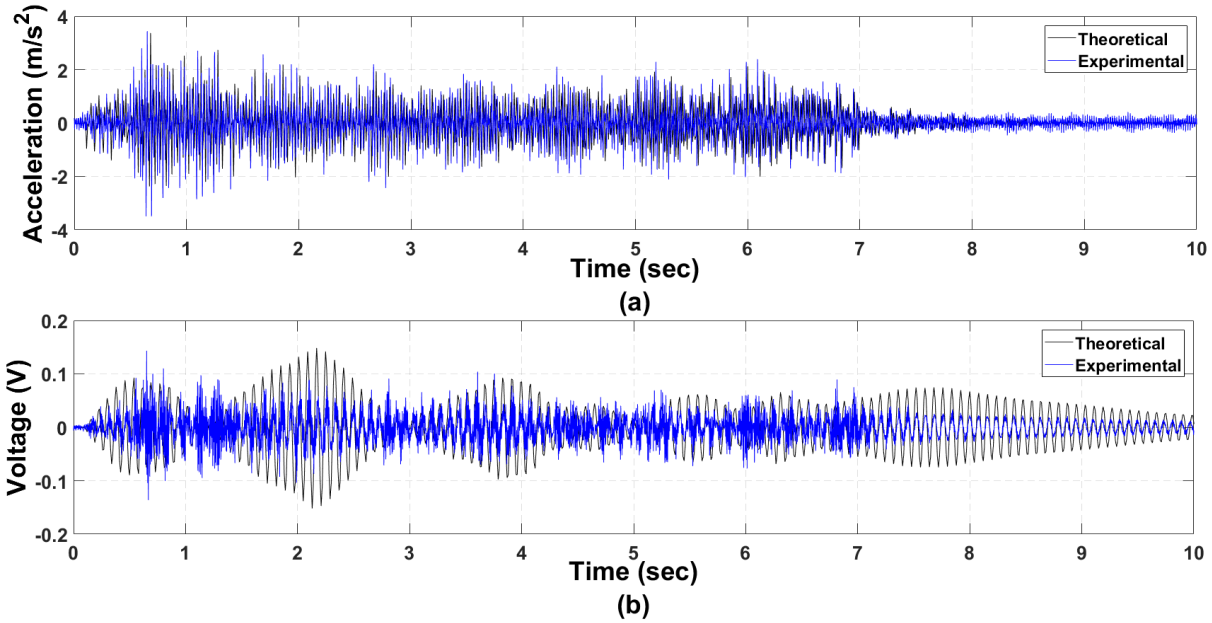

Fig. 7. Comparison of theoretical and laboratory experimental validation for 071Loco train passage including (a) Acceleration and (b) Voltage.

The experimental validation of the EHD for the bridge was subsequently investigated for passages of the 201Loco and TGV trains. The acceleration response of the experimental analysis was in agreement with the theoretical response of the bridge for the passage of the 201Loco [Fig. 8(a)]. The theoretical and experimental voltage outputs were also in agreement, but with noise components in the experimental signals [Fig. 8(b)]. The experimental voltage output from the harvester, $0.140V_{RMS}$, was found to be slightly higher than that obtained theoretically, $0.125V_{RMS}$. The acceleration profile obtained from the bridge response due to the passage of the TGV has good correspondence with the corresponding experimental analysis [Fig. 8(c)]. The peaks at the beginning and the end of the train passage due to the locomotives having a greater magnitude of loading, when compared to the intermediate carriages, are identifiable in both the theoretical and experimental responses. This is also apparent upon the investigation of the theoretical and experimental voltage outputs for the cantilever energy harvester, with peak voltages occurring at the beginning and end of the train passage [Fig. 8(d)]. The voltage output from the theoretical prediction was found to be $0.045V_{RMS}$ and the equivalent experimental voltage output was $0.042V_{RMS}$.

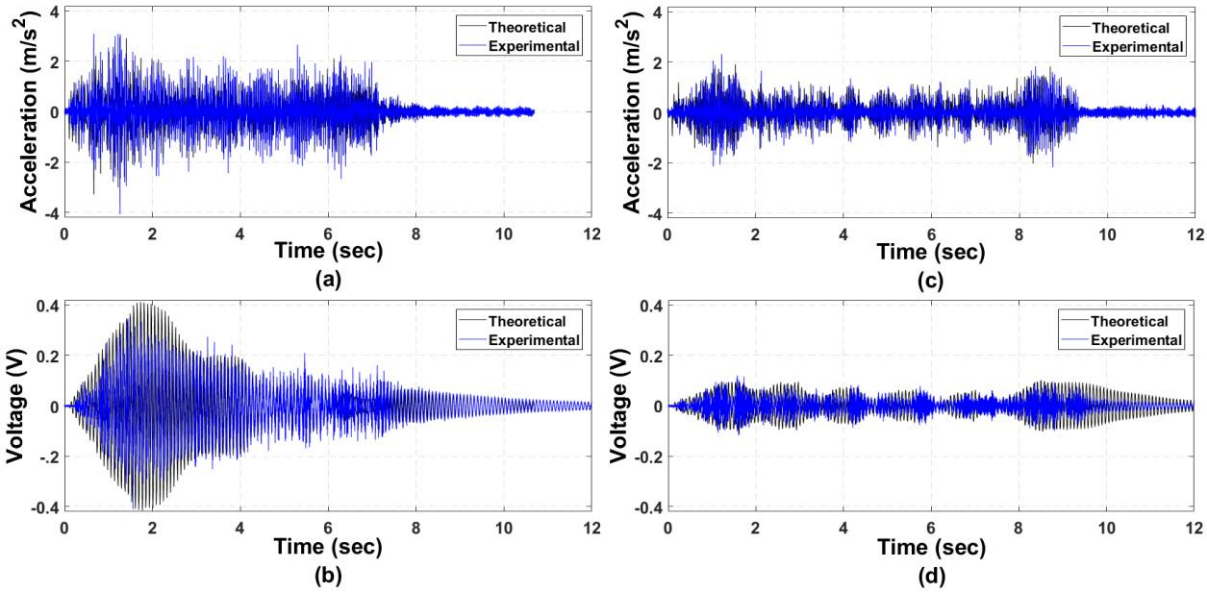

Fig. 8. Comparison of theoretical and laboratory experimental validation for 201Loco train passage including (a) Acceleration and (b) Voltage and TGV passage including (c) Acceleration and (d) Voltage

The final two train passages considered were the ICE and the Shinkansen. It was found that the results from the ICE produced similar to previous results, with the acceleration profiles from both the theoretical analysis and measured experimental analysis showing good match, with the individual axles being detectable in both [Fig. 9(a)]. The voltage outputs from the theoretical and experimental analysis correspond well, with the magnitudes and the profiles being comparable [Fig. 9(b)]. The theoretical voltage output of $0.181V_{RMS}$ compared to an experimental voltage output of $0.183V_{RMS}$. A comparison of the theoretical and experimental outputs of the acceleration response of the bridge to the passage of the Shinkansen shows a good correlation as well with detectable individual axle loads being detectable in both [Fig. 9 (c)] with comparable voltage outputs in experimental and theoretical analysis [Fig. 9(d)]. The voltage output from the theoretical analysis was $0.049V_{RMS}$ and the experimental analysis had a voltage output of $0.042V_{RMS}$. Table 5 summarises the voltage outputs of all five trainsets comparing the theoretical and experimental voltage outputs, including the percentage difference between the two.

	Theory (V_{RMS})	**Experimental (V_{RMS})**	**Difference (%)**
071Loco	0.045	0.037	82.2
201Loco	0.125	0.140	112.0
TGV	0.045	0.042	93.3
ICE	0.181	0.183	101.1
Shinkansen	0.049	0.042	85.7

Table 5. Summary of theoretical and experimental voltage outputs for each train passage

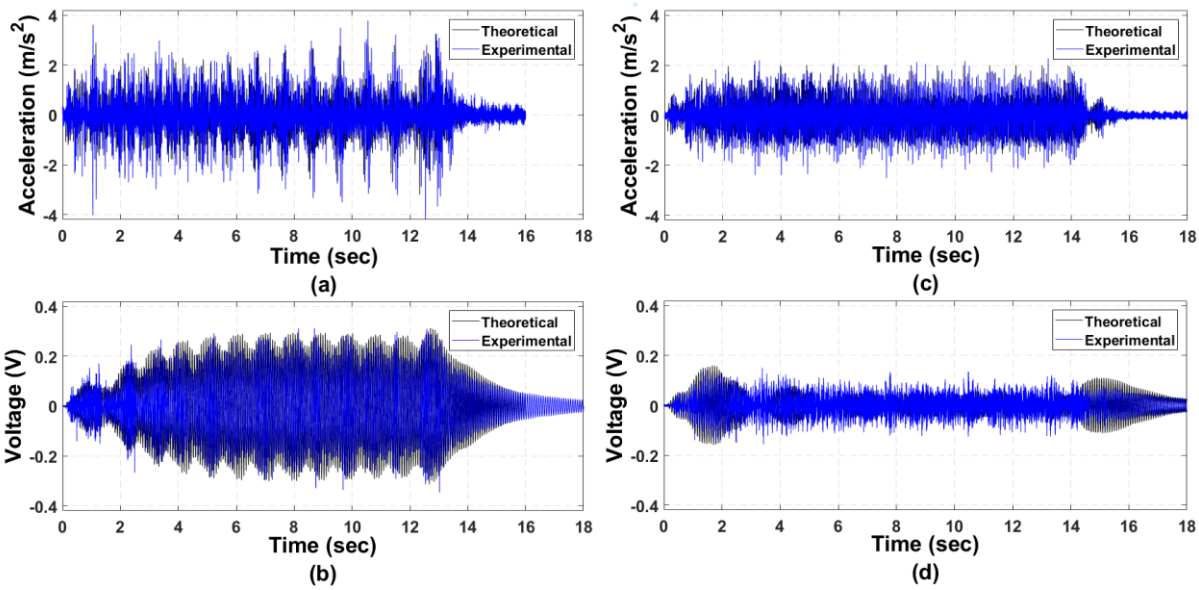

Fig. 9. Comparison of theoretical and laboratory experimental validation for ICE passage including (a) Acceleration and (b) Voltage and Shinkansen passage including (c) Acceleration and (d) Voltage

Analysis of Experimental Validation Results

Following the laboratory experimental validation of the EHD for the bridge structure under different train loading conditions, the results were investigated in the frequency domain. The acceleration and voltage signals of both theoretical and experimental results were compared. The first validation chosen for analysis was the 071Loco, which showed significant similarity between the theoretical and experimental outputs for the acceleration and voltage signals [Fig.10]. When considering acceleration responses, the theoretical and experimental results both showed a peak at the natural frequency of the bridge. A peak at 12.12Hz for the theoretical output compared against 12.03 Hz for the experimental responses [Fig. 10(a)]. The theoretical and experimental signals registered a more notable peak at 39.87Hz and 39.77Hz, respectively. The voltage signals of both the theoretical and experimental were found to have the greatest response between 12Hz and 13.5Hz, around the natural frequency of both the bridge and the harvester [Fig. 10(b)], with peaks of 12.5Hz and 12.68Hz for the theoretical and experimental respectively. As with acceleration response, a large peak was detected in both around 40Hz.

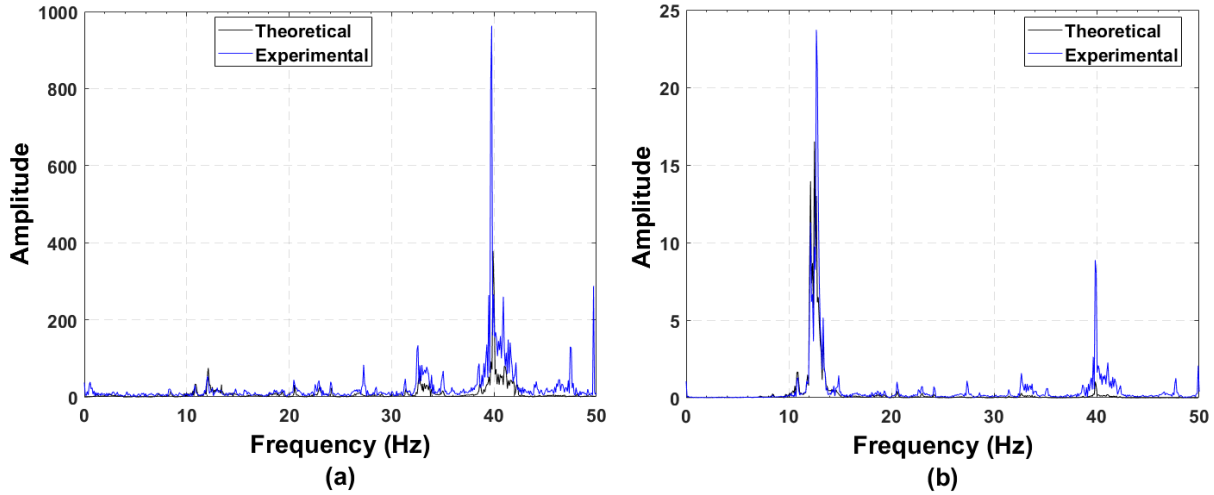

Fig. 10. Analysis of theoretical and experimental outputs due to 071Loco passage from (a) Acceleration outputs and (b) Voltage outputs

Subsequently the experimental validation results for the passages of the 201Loco and the TGV were analyzed and compared against theoretical results [Fig. 11]. It was found that for the 201Loco, the acceleration response of both the theoretical and experimental results are in agreement [Fig. 11(a)]. Peaks at the natural frequency of the bridge were found at 12.54Hz and 12.44Hz, for the theoretical and experimental respectively. As with the 071Loco, the acceleration response of both showed a second peak centered about 40Hz. The voltage response for the passage again showed the frequency domain response peaking around the natural frequency of the bridge and harvester for both theoretical and experimental outputs [Fig. 11(b)], with good correlation between the two. A maximum amplitude occurred at a frequency of 12.53Hz and 12.72Hz for the theoretical and experimental respectively. The TGV passage also had similar levels of correlation between theoretical and experimental results, with the acceleration again detecting the natural frequency of the bridge and peaks centered about 40Hz for both the theoretical and experimental results [Fig. 11(c)]. The voltage response of the EHD showed a peak at the natural frequency, with the maximum amplitude obtained at 12.629Hz for both the theoretical and experimental outputs.

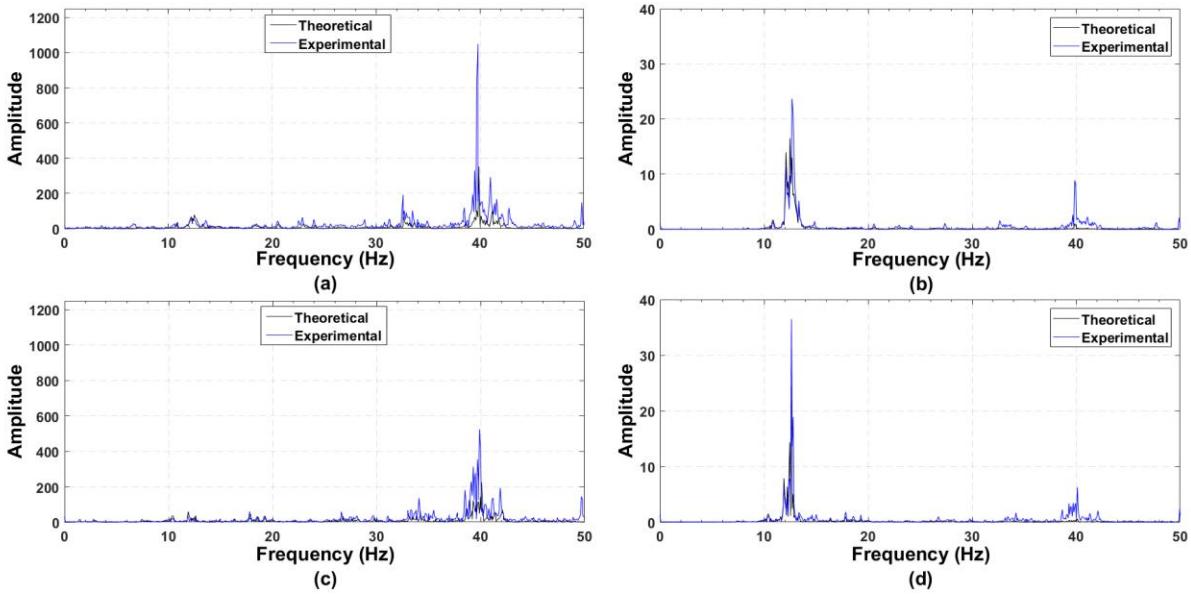

Fig. 11. Analysis of theoretical and experimental outputs due to 201Loco passage for (a) Acceleration and (b) Voltage and TGV passage for (c) Acceleration and (d) Voltage

Of the final two train passages considered, it was found that the ICE resulted in a noisy signal when considering both the theoretical and experimental acceleration outputs [Fig. 12(a)]. The natural frequency of the bridge is evident in both, with the theoretical output having a peak at 12.63Hz and the experimental having a peak at 12.56Hz. Whilst there is again a peak about the 40Hz frequency range, there are further peaks at 23Hz and at 33.50Hz. The voltage analysis of both, however, are in keep with previous results with a peak amplitude found at 12.63Hz and 12.625Hz for the theoretical and experimental results respectively [Fig. 12(b)]. It is noted that while a peak is detectable at 40Hz in both, it is more suppressed when compared against previous train passages. The Shinkansen acceleration results conformed to the results of the first three train passages, with the natural frequency evident at 12.22Hz and 12.16Hz for the theoretical and experimental, respectively, and a peak once again about the 40Hz frequency range [Fig. 12(c)]. The voltage output for both the theoretical and the experimental results, in keeping with all other results, show a maximum amplitude at the natural frequency of the harvester and bridge, with the theoretical obtaining a maximum at 12.22Hz and the experimental at a frequency of 12.71Hz [Fig. 12(d)]. A summary table of all theoretical and experimental frequency outputs for each of the five train passages, with accompanying comparison of the variance between the two, are illustrated in Table 6.

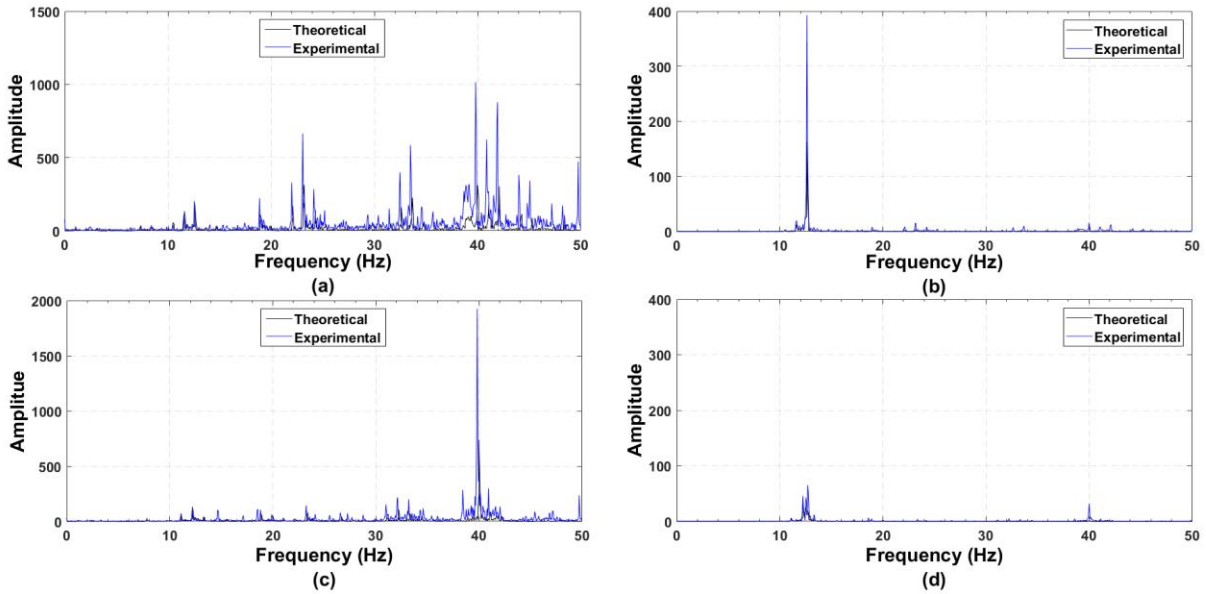

Fig. 12. Analysis of theoretical and experimental outputs due to ICE passage for (a) Acceleration and (b) Voltage and Shinkansen passage for (c) Acceleration and (d) Voltage

	Theory (Hz)	**Experimental (Hz)**	**Difference (%)**
071Loco	12.500	12.689	101.5
201Loco	12.535	12.722	101.5
TGV	12.629	12.629	100.0
ICE	12.625	12.625	100.0
Shinkansen	12.223	12.710	104.0

Table 6. Summary of theoretical and experimental natural frequency for each train passage

CONCLUSIONS

This paper presented a laboratory base experimental methodology for the experimental validation of vibration based energy harvesting devices for built infrastructure in their operational conditions, without having to access the infrastructure. Four critical steps were identified as part of an experimental validation protocol. This comprises of theoretical benchmarking, fabrication, calibration and experimental validation. An experimental setup, through the use of a vibration unit, and the procedure by which individual energy harvesters can be validated for specific structural applications is proposed. The fabrication and calibration of a cantilever piezoelectric energy harvester are outlined for this purpose. A rail bridge traversed by an international train fleet was chosen for developing an experimental evidence base. Experimental results of energy harvesting in the laboratory environment compared well against the numerical estimates in terms of dynamic signatures in time domain, RMS voltages and detection of frequencies of interest. It is expected that the presented study will provide guidance and benchmarking for the experimental validation of piezoelectric energy harvesting devices for civil

infrastructure applications under operational conditions. The study also indicated a method where historical data can be used to validate and estimate conditions of implementation and designs of harvesters for implementation on the same or a different site.

REFERENCES

Ali, S. F., Friswell, M. I. and Adhikari, S. (2011). "Analysis of energy harvesters for highway bridges." *J. Intell. Material Syst. Struct.*, **22**(16), 1929–1938. DOI: https://doi.org/10.1177/1045389X11417650

Al-Ashtari, W., Hunstig, M., Hemsel, T. and Sextro, W. (2013). "Enhanced energy harvesting using multiple piezoelectric elements: theory and experiments." *Sens. Actuators A Phys.*, 200, 138-146. DOI: https://doi.org/10.1016/j.sna.2013.01.008

Anton, S. R. and Sodano, H. A. (2007). "A review of power harvesting using piezoelectric materials (2003–2006)." *Smart Mater. Struct.*, 16(3), R1– R21. DOI: https://doi.org/10.1088/0964-1726/16/3/R01

Cahill, P., Hanley, C., Jaksic, V., Mathewson, A. and Pakrashi, V. (2016a). "Energy harvesting for monitoring bridges over their operational life." *Proc., 8th Eur., Wksk., Struct. Health Mon. (EWSHM)*, Bilbao, Spain, 11 pp. URL: https://cora.ucc.ie/bitstream/handle/10468/3352/1845.pdf?sequence=1&isAllowed=y

Cahill, P., Jaksic, V., Keane, J., O'Sullivan, A., Mathewson, A., Ali, S. F. and Pakrashi, V. (2016b). "Effect of Road Surface, Vehicle, and Device Characteristics on Energy Harvesting from Bridge–Vehicle Interactions', Comput. -Aided Civ. Infrastruct. Eng., **31**(12), 921-935. DOI: https://doi.org/10.1111/mice.12228

Cahill, P., O'Keeffe, R., Jackson, N., Mathewson, A. and Pakrashi, P. (2014a). "Structural Health Monitoring of Reinforced Concrete Beam Using Piezoelectric Energy Harvesting System." *Proc., 7th Eur., Wksk., Struct. Health Mon. (EWSHM)*, Nantes, France, 7 pp. URL: https://hal.archives-ouvertes.fr/hal-01020338/document

Cahill, P., Nuallain, N. A. N., Jackson, N., Mathewson, A., Karoumi, R. and Pakrashi, V. (2014b). "Energy harvesting from train-induced response in bridges." *J. Bridge Eng.*, 10.1061/(ASCE)BE.1943-5592.0000608, 04014034. DOI: https://doi.org/10.1061/(ASCE)BE.1943-5592.0000608

Chong C.-Y. and Kumar, S. (2003). "Sensor networks: Evolution, opportunities, and challenges." *Proc. IEEE*, **91**(8), 1247–1256. DOI: https://doi.org/10.1109/JPROC.2003.814918

DuToit, N. E. and Wardle, B. L. (2007). "Experimental verification of models for microfabricated piezoelectric vibration energy harvesters." *AIAA Journal*, **45**(5), 1126–1137. DOI: http://dx.doi.org/10.2514/1.25047

Erturk, A. (2011). "Piezoelectric energy harvesting for civil infrastructure system applications: Moving loads and surface strain fluctuations." *J. Intell. Material Syst. Struct.*, **22**(17), 1959–1973. DOI: https://doi.org/10.1177/1045389X11420593

Gungor, V. and Hancke, G. (2009). "Industrial wireless sensor networks: Challenges, design principles, and technical approaches." *IEEE Trans. Ind. Electron.*, 56(10), 4258–4265. DOI: 10.1109/TIE.2009.2015754

IEEE (The Institute of Electrical and Electronics Engineers). (1988). "Standard on Piezoelectricity." ANSI/IEEE Std 176-1987, New York.

Jackson, N., Keeney, L. and Mathewson, A. (2013). "Flexible-CMOS and biocompatible piezoelectric AlN material for MEMS applications." *Smart Mater. Struct.*, 22(11), 115033. DOI: https://doi.org/10.1088/0964-1726/22/11/115033

Kaur, N. and Bhalla, S. (2016). "Numerical investigations on energy harvesting potential of thin PZT patches adhesively bonded on RC structures." *Sens. Actuators A Phys.*, **241**, 44-59. DOI: https://doi.org/10.1016/j.sna.2016.02.002

Kim, S-H., Ahn, J-H., Chung, H-M. and Kany, H-W. (2011). "Analysis of piezoelectric effects on various loading conditions for energy harvesting in a bridge system." *Sens. Actuators A Phys.*, **167**, 468-483. DOI: https://doi.org/10.1016/j.sna.2011.03.007

Kołakowski, P., Szelążek, J., Sekuła, K., Świercz, A., Mizerski, K. and Gutkiewicz, P. (2011). "Structural health monitoring of a railway truss bridge using vibration-based and ultrasonic methods." *Smart Mater. Struct.*, **20**(3), 035016. DOI: https://doi.org/10.1088/0964-1726/20/3/035016

Liu, H., Lee, C., Kobayashi, T., Tay, C. J., and Quan, C. (2012). "Piezoelectric MEMS-based wideband energy harvesting systems using a frequency-up-conversion cantilever stopper." *Sens. Actuators A Phys.*, **186**, 242-248. DOI: https://doi.org/10.1016/j.sna.2012.01.033

435 Pakrashi, V., Harkin, J. and Kelly, J, (2013). "Monitoring and repair of an impact damaged prestressed bridge."
436 *Pro. ICE – J. Bridge Eng.*, **166**, 16–29. DOI: http://dx.doi.org/10.1680/bren.10.00057

437 Peigney, M. and Siegert, D. (2013). "Piezoelectric energy harvesting from traffic induced bridge vibrations."
438 *Smart Mater. Struct.*, **22**(9), 095019. DOI: https://doi.org/10.1088/0964-1726/22/9/095019

439 Priya, S. (2007). "Advances in energy harvesting using low profile piezoelectric transducers." *J. Electroceram.*,
440 **19**(1), 167–184. DOI: https://doi.org/10.1007/s10832-007-9043-4

441 Sazonov, E., Curry, D. and Pillay, P. (2009). "Self-powered sensors for monitoring of highway bridges." *IEEE*
442 *Sens. J.*, **9**(11), 1422–1429. DOI: https://doi.org/10.1109/JSEN.2009.2019333

443 Shaikh, F. K. and Zeadally, S. (2016). "Energy harvesting in wireless sensor networks: A comprehensive review."
444 *Renew. Sust. Energ. Rev.*, 55, 1041-1054. DOI: https://doi.org/10.1016/j.rser.2015.11.010

445 Wang, H and Meng, Q. (2013). 'Analytical modeling and experimental verification of vibration-based piezoelec-
446 tric bimorph beam with a tip-mass for power harvesting', *Mech. Syst. Signal Process.*, **36(1)**, 193-209. DOI:
447 https://doi.org/10.1016/j.ymssp.2012.10.015

448 Wischke, M., Masur, M., Kröner, M. and Woias, P. (2011). "Vibration harvesting in traffic tunnels to power
449 wireless sensor nodes." *Smart Mater. Struct.*, **20**(8), 085014. DOI: https://doi.org/10.1088/0964-
450 1726/20/8/085014

451 Xie, X. D., Wu, N., Yuen, K. V. and Wang, Q. (2013). "Energy harvesting from high-rise buildings by a piezoe-
452 lectric coupled cantilever with a proof mass." *Int. J. Eng. Sci.*, **72**, 98–106. DOI: https://doi.org/10.1016/j.ijeng-
453 sci.2013.07.004

454 Znidaric, A., Pakrashi, V., O'Connor, A. and O'Brien, E. (2011). "A Review of Road Structure Data in Six Euro-
455 pean Countries." *Pro. ICE – J. Urban Design Plan.*, **164**(4), 225-232. DOI: http://dx.doi.org/10.1680/udap.900054

456 Zuo, L. and Tang, X. (2013). "Large-scale vibration energy harvesting." *J. Intell. Material Syst. Struct.*, **24**(11),
457 1405-1430. DOI: https://doi.org/10.1177/1045389X13486707